Inorganica Chimica Acta 544 (2023) 121239

Contents lists available at ScienceDirect

Inorganica Chimica Acta

journal homepage: www.elsevier.com/locate/ica

Novel PEPPSI-type *N*-heterocyclic carbene palladium(II) complexes: Synthesis, characterization, *in silico* studies and enzyme inhibitory properties against some metabolic enzymes

Beyhan Yiğit [a], Parham Taslimi [b], Duygu Barut Celepci [c], Tuğba Taskin-Tok [d,e], Murat Yiğit [f,*], Muhittin Aygün [c], İsmail Özdemir [g,h,i], İlhami Gülçin [j]

[a] Department of Chemistry, Faculty of Science and Art, Adiyaman University, 02040 Adıyaman, Turkey
[b] Department of Biotechnology, Faculty of Science, Bartin University, 74100 Bartin, Turkey
[c] Department of Physics, Faculty of Science, Dokuz Eylül University, 35160 İzmir, Turkey
[d] Gaziantep University, Faculty of Arts and Sciences, Department of Chemistry, Gaziantep, Turkey
[e] Gaziantep University, Institute of Health Sciences, Department of Bioinformatics and Computational Biology, Gaziantep, Turkey
[f] Department of Chemistry and Chemical Process Technologies, Vocational School of Technical Sciences, Adiyaman University, 02040 Adıyaman, Turkey
[g] Department of Chemistry, Faculty of Science and Art, İnönü University, 44280 Malatya, Turkey
[h] Catalysis Research and Application Center, İnönü University, 44280 Malatya, Turkey
[i] Drug Application and Research Center, İnönü University, 44280 Malatya, Turkey
[j] Department of Chemistry, Faculty of Science, Atatürk University, 25240 Erzurum, Turkey

ARTICLE INFO

Keywords:
N-heterocyclic carbene
Palladium(II)-PEPPSI complexes
Enzymes inhibition
Molecular docking
Single-crystal X-ray

ABSTRACT

In this study, a series of PEPPSI-type *N*-heterocyclic carbene palladium(II) complexes **3a-e** were synthesized using amine functionalized benzimidazolium salts **2a-e** as *N*-heterocyclic carbene precursors. These complexes were characterized by FT-IR, ^{1}H NMR and ^{13}C NMR spectroscopy, elemental analysis and mass spectrometry. Also, the molecular and crystal structure of **3b** has been determined by the single-crystal X-ray diffraction method. According to the structural analysis, the geometry of the palladium center of the complex adopts a slightly distorted square planar environment. The benzimidazolium salts **2a-e** and their palladium(II) complexes **3a-e** were screened for human carbonic anhydrase I, II (hCAs I and II), and α-glycosidase inhibitory activities. Results indicated that all the synthetic compounds exhibited potent inhibitory activities against all targets as compared to the standard inhibitors, revealed by IC_{50} values. K_i values of **2a-e** and **3a-e** for hCA I, hCA II, and α-glycosidase enzymes were obtained in the ranges 1.17 ± 0.11–65.50 ± 8.20 μM, 1.02 ± 0.08–57.60 ± 6.41 μM, and 118.86 ± 11.92–509.21 ± 26.61 nM, respectively. Besides these, molecular docking calculations of potent compounds **2b, 2d, 2e, 3a, 3b, 3c** and **3e** towards human carbonic anhydrase I (hCA I), human carbonic anhydrase II (hCA II), and α-glycosidase (α-Gly) were presented using AutoDock 4. Among the compounds discussed, compounds **3c, 3a, 2e** and **2b** have the best binding affinity for α-Gly (-9.87, −9.77, −9.04 and −8.63 kcal/mol); compounds **3e, 3b, 2d** and **2e** turn out to have the second-best binding affinity (-8.80, −8.74, −8.39 and −7.57 kcal/mol) against hCA II. Lastly, compounds showing the lowest binding affinity for hCA I enzyme are **3e, 3b, 2d** and **2e**, respectively. These findings show that especially NHC-palladium(II) complexes **3a-e** are more active for all three enzyme structures than their *N*-heterocyclic carbene precursors **2a-e** and may be potential candidates for the discovery and development of effective inhibitors for the related enzymes in the future.

1. Introduction

N-Heterocyclic carbenes (NHCs) are neutral, two electron donor ligands, which have strong σ-donating and weak π-accepting abilities. Also, they have unique properties such as lower toxicity, electronic and steric tunability, ease of synthesis and structural modification and tight binding to the metals [1]. Therefore, NHCs have been one of the most exploited classes of ligands for the synthesis of transition metal complexes in the last few decades. The first examples of *N*-heterocyclic carbene metal complexes were independently reported by Öfele [2] and

* Corresponding author.
E-mail address: myigit@adiyaman.edu.tr (M. Yiğit).

https://doi.org/10.1016/j.ica.2022.121239
Received 6 July 2022; Received in revised form 2 October 2022; Accepted 2 October 2022
Available online 6 October 2022

Wanzlick in 1968 [3]. Metal complexes of NHC ligands were extensively studied in 1970 s by Lappert and co-workers [4]. In 1991, Arduengo and co-workers successfully isolated and characterized the first stable free *N*-heterocyclic carbene [5]. The use of palladium-NHC complexes as catalysts for Heck reactions was demonstrated by Herrmann in 1995 [6]. The first studies on the medicinal applications of metal-NHC complexes were reported by Çetinkaya and co-workers in 1996 [7]. Since then, different types of NHCs, such as imidazolin-2-ylidenes, benzimidazolin-2-ylidenes, imidazolidin-2-ylidenes and 1,2,4-triazolin-5-ylidenes have been successfully synthesized and used as ligands in organometallic chemistry, medicinal chemistry and catalysis [8–13]. Benzimidazolium salts are the most widely used precursors for the synthesis of NHC complexes [14–17]. Also, these salts have a wide range of applications such as ionic liquids, fluorescence sensors, and solar cells [18–20]. In recent years, benzimidazolium salts and corresponding NHC complexes have been most often studied for their potential bioactivities including anticancer, antitumor and antimicrobial activities [21–23]. For example, Morales-Morales and co-workers reported the synthesis and in vitro anticancer activity of a series of benzimidazolium salts and their Ir-NHC complexes. They demonstrated that the Ir complexes exhibited better activity in comparison with the corresponding NHC precursors [24]. Palladium complexes of NHC ligands have been widely used as precatalysts in a wide range of carbon–carbon and carbon-heteroatom bond formation reactions [25–28]. Palladium complexes bearing a bulky NHC, two halides (X) and pyridine (Py) ligands (NHC-PdX_2-Py), commonly known as the PEPPSI (Pyridine-Enhanced Precatalyst, Preparation, Stabilization and Initiation) complex were first reported by Organ in 2006 [29]. Since then, PEPPSI-themed (NHC)PdX_2(pyridine) complexes have been attracting much interest because of their wide applicability in catalysis [30–33]. Besides their use as catalysts, metal-NHC complexes also proved to be promising structures for biological applications [34,35]. Over the last few decades, NHC complexes have been extensively studied biologically [36–38]. Especially, metal-NHC complexes containing Ag, Au, Cu, Ru, Rh, Pd and Pt have been explored as efficient antibacterial and anticancer agents against numerous bacterial species and various cancer cell lines [39–44]. Among them, Au and Ag complexes have shown promising anticancer and antimicrobial properties [45–49]. Pd(II) complexes, which are structurally similar to Pt(II) complexes have much interest as potential anticancer agents. For example, Ghosh and co-workers have reported the Pd complexes, (NHC)Pd(pyridine)Cl_2 and $(NHC)_2PdCl_2$, that display strong cytotoxicity against human tumor cell lines (HeLa, MCF-7, HCT 116) in vitro [50]. In recent years, PEPPSI-type NHC-Pd(II) complexes have been examined as enzyme inhibitors by Gülçin and co-workers, and studies showed that these complexes possess inhibitory potential against metabolic enzymes [51–53].

Carbonic anhydrase (CA) enzyme; Amino acids are classified into different groups due to their different sequence, folding, and composition of different building blocks. It is generally classified into eight gene families, namely "α-, β-, γ-, δ-, ζ-, η-, θ- and *t*-CAs" [54,55]. The catalytic mechanism of the CA enzyme has been tried to be clarified since it has advantageous properties such as being very important in the metabolism of the CA enzyme, being stable in the solution environment and being able to be kept for a long time without losing its activity under suitable conditions. As a result, it has been determined that the CA enzyme has two important structural features: it contains Zn^{2+} ions and a hydroxyl group attached to it in the active site also amino acids near the active site are coordinated to form a proton gradient and a proton donor [56,57]. The hCA I is an isoenzyme found in human erythrocyte cells. This isoenzyme is involved in respiration. The hCA II isoenzyme is a very important enzyme for bone, brain and kidney tissues. Compared to the hCA I isoenzyme, it is found in lesser amounts in humans. The hCA II isoenzyme ensures the reabsorption of Na^+ and water in the renal cortex; for this reason, kidney stones, bone and calcification in the brain occur in its deficiency [58]. The hCA II enzyme is found in most cells, while hCA I is specific for erythrocytes [59]. Additionally, α-glycosidases at the mucosal brush border of the small intestine catalyze the digestion of starch and disaccharides, which are predominant in the human regimen. The α-glycosidase enzymes located in the small intestine brush border are especially capable of hydrolyzing terminal 1 → 4-linked glucose residues to release a single α-glucose molecule [60–62].

In a recent study, we reported the synthesis of dimethylamine-functionalized benzimidazolium salts, which demonstrated good inhibition effects against metabolic enzymes [63]. In another study, Özdemir and co-workers reported the silver(I)–NHC and gold(I)–NHC complexes bearing diisopropylamine group that showed anticancer activity against human cell lines, namely brain (SHSY5Y), colon (HTC 116), and liver (HEP3B) [64]. In the present study, the diisopropylamine-tethered benzimidazolium salts and corresponding (NHC)PdX_2(pyridine) complexes were synthesized and tested against the metabolic enzymes. Biological evaluation of the activities of benzimidazolium salts (**2b, 2d** and **2e**) and palladium complexes (**3a, 3b, 3c** and **3e**) against hCA I, hCA II, and α-Gly within the scope of this study was also made with help of molecular docking.

2. Experimental

2.1. Materials and methods

All reactions for the preparation of the benzimidazolium salts and NHC-palladium(II)-PEPPSI complexes were carried out under air. Chemicals and solvents were purchased from Sigma-Aldrich and used as received. Benzimidazolium salts (**2a-e**) were prepared according to procedures described in the literature [10,65]. ^{1}H NMR and ^{13}C NMR spectra were recorded with a Varian AS 400 Merkur spectrometer operating at 400 MHz (^{1}H), 100 MHz (^{13}C) in $CDCl_3$ with tetramethylsilane as an internal reference. ^{1}H peaks were labeled as singlet (s), doublet (d), triplet (t), septet (sept.) and multiplet (m). Chemical shifts and coupling constants (*J* values) were reported in ppm and in Hz, respectively. FT-IR spectra were recorded on the ATR unit in the range 400–4000 cm^{-1} on Perkin Elmer Spectrum 100. The mass spectrometric analysis was performed at the Thermo Scientific Exactive Plus Benchtop Full-Scan Orbitrap Mass Spectrometer LC-MS/MS analyzer. Elemental analyses were obtained with a LECO CHNS-932 elemental analyzer. Melting points were measured in open capillary tubes with Stuart SMP 40 melting point apparatus and uncorrected.

2.2. General procedure for the preparation of the benzimidazolium salts, *2a-e*

To a solution of 1-(2-diisopropylaminoethyl)benzimidazole (10.00 mmol) in N,*N*-dimethylformamide (5 mL), alkyl chloride (10.15 mmol) was added. The reaction mixture was stirred at room temperature for 2 h and heated at 80 °C for 18 h. After the reaction completed, the reaction mixture was cooled to room temperature. Diethyl ether (10 mL) was added to obtain a white crystalline solid, which was filtered off. The solid was washed with diethyl ether and dried under vacuum. The crude product was recrystallized from ethanol/diethyl ether to give of white crystals.

2.3. General procedure for the preparation of the palladium complexes, *3a-e*

A mixture of benzimidazolium salt (0.30 g, 0.73 mmol), $PdCl_2$ (0.13 g, 0.73 mmol) and K_2CO_3 (0.50 g, 3.65 mmol) in pyridine (3 mL) was heated with vigorous stirring at 80 °C for 10 h. Upon completion of the reaction, the pyridine was removed by vacuum distillation and dichloromethane (20 mL) was added to the residue. The obtained mixture was filtered into a silica gel column and then the solvent was removed under reduced pressure. The product was recrystallized from dichloromethane / diethyl ether at room temperature. The resulting

bright yellow crystals were isolated by filtration and dried in vacuum.

2.3.1. Dichloro[1-(2-diisopropylaminoethyl)-3-(benzyl)benzimidazol-2-ylidene]pyridinepalladium(II), **3a**

Yield: 0.36 g, 84 %, m.p.: 182–183 °C, IR: $\nu_{(NCN)}$ = 1411.7 cm^{-1}. ^1H NMR ($CDCl_3$) δ: 8.99 (d, 2H, *J* = 4.0 Hz, pyridine-*H*), 7.77 (t, 1H, *J* = 4.0 Hz, pyridine-*H*), 7.06–7.58 (m, 11*H*, NC_6H_4N, $CH_2C_6H_5$ and pyridine-*H*), 6.21 (s, 2H, $CH_2C_6H_5$), 4.88 (t, 2H, *J* = 8.0 Hz, $CH_2CH_2N(^iPr)_2$), 3.27 (t, 2H, *J* = 8.0 Hz, $CH_2CH_2N(^iPr)_2$), 3.17 (sept, 2H, *J* = 8.0 Hz, $NCH(CH_3)_2$), 1.17 (d, 12H, *J* = 8.0 Hz, $NCH(CH_3)_2$). ^{13}C NMR ($CDCl_3$) δ: 163.90 (Pd-$C_{carbene}$), 151.22, 138.09, 135.11, 135.06, 134.01, 128.84, 128.13, 127.97, 124.49, 123.13, 123.06, 111.44, 110.52 (NC_6H_4N, $CH_2C_6H_5$ and pyridine-*C*), 53.18 ($CH_2C_6H_5$), 50.02 ($CH_2CH_2N(^iPr)_2$), 49.89 ($NCH(CH_3)_2$), 44.87 ($CH_2CH_2N(^iPr)_2$), 21.17 ($NCH(CH_3)_2$). Anal. Calcd. for $C_{27}H_{34}N_4Cl_2Pd$: C, 54.78; H, 5.75; N, 9.47. Found: C, 54.91; H, 5.54; N, 9.36. HR-AM (*m/z*): Calcd for $C_{22}H_{29}N_3Pd$ $[M-Py-2Cl-H]^+$: 440.1396, found: 440.1290.

2.3.2. Dichloro[1-(2-diisopropylaminoethyl)-3-(2-methylbenzyl) benzimidazol-2-ylidene]pyridinepalladium(II), **3b**

Yield: 0.30 g, 68 %, m.p.: 169–171 °C, IR: $\nu_{(NCN)}$ = 1404.9 cm^{-1}. ^1H NMR ($CDCl_3$) δ: 8.88 (d, 2H, *J* = 4.0 Hz, pyridine-*H*), 7.69 (t, 1H, *J* = 8.0 Hz, pyridine-*H*), 6.85–7.40 (m, 10*H*, NC_6H_4N, $CH_2C_6H_4(CH_3)$-2 and pyridine-*H*), 6.09 (s, 2H, $CH_2C_6H_4(CH_3)$-2), 4.82 (t, 2H, *J* = 8.0 Hz, $CH_2CH_2N(^iPr)_2$), 3.20 (t, 2H, *J* = 8.0 Hz, $CH_2CH_2N(^iPr)_2$), 3.09 (sept, 2H, *J* = 4.0 Hz, $NCH(CH_3)_2$), 2.43 (s, 3H, $CH_2C_6H_4(CH_3)$-2), 1.10 (d, 12H, *J* = 4.0 Hz, $NCH(CH_3)_2$). ^{13}C NMR ($CDCl_3$) δ: 163.17 (Pd-$C_{carbene}$), 150.16, 137.04, 134.36, 133.94, 133.09, 131.89, 129.34, 127.04, 126.89, 125.48, 123.43, 122.11, 110.19, 109.58 (NC_6H_4N, $CH_2C_6H_4(CH_3)$-2 and pyridine-*C*), 49.29 ($CH_2C_6H_4(CH_3)$-2), 49.05 ($CH_2CH_2N(^iPr)_2$), 48.84 ($NCH(CH_3)_2$), 43.89 ($CH_2CH_2N(^iPr)_2$), 20.14 ($NCH(CH_3)_2$), 18.72 $CH_2C_6H_4(CH_3)$-2). Anal. Calcd. for $C_{28}H_{36}N_4Cl_2Pd$: C, 55.50; H, 5.95; N, 9.25. Found: C, 55.71; H, 5.78; N, 9.44. HR-AM (*m/z*): Calcd for $C_{23}H_{31}N_3Pd$ $[M-Py-2Cl-H]^+$: 454.1553, found: 454.1441.

2.3.3. Dichloro[1-(2-diisopropylaminoethyl)-3-(2,4,6-trimethylbenzyl) benzimidazol-2-ylidene]pyridinepalladium(II), **3c**

Yield: 0.33 g, 72 %, m.p.: 209–210 °C, IR: $\nu_{(NCN)}$ = 1403.3 cm^{-1}. ^1H NMR ($CDCl_3$) δ: 8.99 (d, 2H, *J* = 4.0 Hz, pyridine-*H*), 7.79 (t, 1H, *J* = 8.0 Hz, pyridine-*H*), 6.92–7.41 (m, 8H, NC_6H_4N, $CH_2C_6H_2(CH_3)_3$–2,4,6 and pyridine-*H*), 6.21 (s, 2H, $CH_2C_6H_2(CH_3)_3$–2,4,6), 4.87 (t, 2H, *J* = 8.0 Hz, $CH_2CH_2N(^iPr)_2$), 3.25 (t, 2H, *J* = 8.0 Hz, $CH_2CH_2N(^iPr)_2$), 3.16 (sept, 2H, *J* = 8.0 Hz, $NCH(CH_3)_2$), 2.34 (s, 3H, $CH_2C_6H_2(CH_3)_3$–4), 2.33 (s, 6H, $CH_2C_6H_2(CH_3)_3$–2,6), 1.17 (d, 12H, *J* = 8.0 Hz, $NCH(CH_3)_2$). ^{13}C NMR ($CDCl_3$) δ: 163.46 (Pd-$C_{carbene}$), 153.34, 151.20, 138.82, 138.59, 138.55, 138.06, 134.88, 134.36, 129.55, 127.44, 124.98, 124.48, 123.00, 122.70, 111.43, 110.28 (NC_6H_4N, $CH_2C_6H_2(CH_3)_3$–2,4,6 and pyridine-*C*), 50.13 ($CH_2C_6H_2(CH_3)_3$–2,4,6), 49.97 ($CH_2CH_2N(^iPr)_2$), 49.89 ($NCH(CH_3)_2$), 44.84 ($CH_2CH_2N(^iPr)_2$), 21.10, 21.16 ($CH_2C_6H_2(CH_3)_3$–2,4,6), 20.72 ($NCH(CH_3)_2$). Anal. Calcd. for $C_{30}H_{40}N_4Cl_2Pd$: C, 56.84; H, 6.32; N, 8.84. Found: C, 56.78; H, 6.35; N, 8.77. HR-AM (*m/z*): Calcd for $C_{25}H_{35}N_3Pd$ $[M-Py-2Cl-H]^+$: 482.1866, found: 482.1753.

2.3.4. Dibromo[1-(2-diisopropylaminoethyl)-3-(4-tertbutylbenzyl) benzimidazol-2-ylidene]pyridinepalladium(II), **3d**

Yield: 0.44 g, 81 %, m.p.: 190–192 °C, IR: $\nu_{(NCN)}$ = 1409.1 cm^{-1}. ^1H NMR ($CDCl_3$) δ: 9.00 (d, 2H, *J* = 4.0 Hz, pyridine-*H*), 7.75–7.83 (m, 1H, *J* = 8.0 Hz, pyridine-*H*), 7.09–7.54 (m, 10*H*, NC_6H_4N, $CH_2C_6H_4C(CH_3)_3$–4, pyridine-*H*), 6.10 (s, 2H, $CH_2C_6H_4C(CH_3)_3$–4), 5.71–5.79 (m, 2H, $CH_2CH_2N(^iPr)_2$), 3.83–3.98 (m, 2H, $CH_2CH_2N(^iPr)_2$), 3.83–3.98 (m, 2H, $NCH(CH_3)_2$), 1.63 (s, 9H, $CH_2C_6H_4C(CH_3)_3$–4), 1.28 (d, 12H, *J* = 4.0 Hz, $NCH(CH_3)_2$). ^{13}C NMR ($CDCl_3$) δ: 163.40 (Pd-$C_{carbene}$), 154.30, 152.42, 151.34, 138.40, 138.24, 134.64, 134.17, 131.29, 128.33, 127.83, 126.39, 125.82, 125.03, 124.78, 123.70, 113.38, 111.66 (NC_6H_4N, $CH_2C_6H_4C(CH_3)_3$–4 and pyridine-*C*), 65.86 ($CH_2C_6H_4C(CH_3)_3$–4), 54.70 ($CH_2CH_2N(^iPr)_2$), 53.52 ($NCH(CH_3)_2$), 44.37 ($CH_2CH_2N(^iPr)_2$), 34.60 ($CH_2C_6H_4C(CH_3)_3$–4), 31.29, 31.18 ($CH_2C_6H_4C(CH_3)_3$–4), 18.81 ($NCH(CH_3)_2$). Anal. Calcd. for $C_{31}H_{42}N_4Br_2Pd$: C, 50.52; H, 5.70; N, 7.60. Found: C, 50.58; H, 5.75; N, 7.69. HR-AM (*m/z*): Calcd for $C_{26}H_{37}N_3Pd$ $[M-Py-2Br-H]^+$: 496.2022, found: 496.1911.

2.3.5. Dibromo[1-(2-diisopropylaminoethyl)-3-(benzhydryl)benzimidazol-2-ylidene]pyridinepalladium(II), **3e**

Yield: 0.39 g, 71 %, m.p.: 202–204 °C, IR: $\nu_{(NCN)}$ = 1403.0 cm^{-1}. ^1H NMR ($CDCl_3$) δ: 8.95 (d, 2H, *J* = 4.0 Hz, pyridine-*H*), 7.71 (t, 1H, *J* = 8.0 Hz, pyridine-*H*), 6.76–7.48 (m, 17H, NC_6H_4N, $CH(C_6H_5)_2$ and pyridine-*H*), 4.81–4.91 (m, 2H, $CH_2CH_2N(^iPr)_2$), 3.26–3.32 (m, 2H, $CH_2CH_2N(^iPr)_2$), 3.13–3.19 (m, 2H, $NCH(CH_3)_2$), 1.18 (d, 12H, *J* = 4.0 Hz, $NCH(CH_3)_2$). ^{13}C NMR ($CDCl_3$) δ: 167.70 (Pd-$C_{carbene}$), 154.32, 152.66, 152.53, 137.78, 137.45, 134.63, 133.96, 129.16, 129.09, 128.52, 128.48, 128.07, 125.00, 124.54, 124.47, 122.51, 113.60, 113.50 (NC_6H_4N, $CH(C_6H_5)_2$ and pyridine-*C*), 68.44 ($CH(C_6H_5)_2$), 50.00 ($CH_2CH_2N(^iPr)_2$), 49.94 ($NCH(CH_3)_2$), 44.23 ($CH_2CH_2N(^iPr)_2$), 21.23 ($NCH(CH_3)_2$). Anal. Calcd. for $C_{33}H_{38}N_4Br_2Pd$: C, 52.35; H, 5.02; N, 7.40. Found: C, 52.44; H, 5.05; N, 7.36. HR-AM (*m/z*): Calcd for $C_{28}H_{33}N_3Pd$ $[M-Py-2Br-H]^+$: 516.1709, found: 516.1601.

2.4. X-ray crystallography

A suitable single-crystal of PEPPSI complex **3b** was selected for data collection and performed on Rigaku Oxford Xcalibur X-ray diffractometer at room temperature (294 K) with EOS CCD area detector using graphite-monochromated MoKα radiation (λ = 0.71073 Å) with ω-scan mode. Crystal data collection, data reduction and analytical absorption corrections were accomplished using the CrysAlisPro software v. 1.171.41.93a [66,67]. Using OLEX2 as the graphical interface, the structure was solved by the ShelXT structure solution program, employing the *Intrinsic Phasing* method [68]. The model was refined by the full-matrix least-squares method based on F^2 against all reflections with SHELXL [68]. All non-hydrogen atoms were refined anisotropically and hydrogen atoms were added to the structure in idealized positions and further refined according to the riding model (the aromatic C—H = 0.93 Å, the methylene C—H = 0.97 Å, and the methyl C—H = 0.96 Å). Geometrical calculations were performed using PLATON software [69] and molecular graphics were generated using OLEX2 version 1.2 [70]. Table S1 summarizes the processes of data collection and refinement of the complex. CCDC entry code 2,156,701 contains the supplementary crystallographic data for this paper. These data can be obtained free of charge at http://www.ccdc.cam.ac.uk/conts/retrieving.html or from the Cambridge Crystallographic Data Center, 12, Union Road, Cambridge CB2 1EZ, UK. Fax: (+44) 1223–336-033, email: deposit@ccdc.cam.ac.uk.

2.5. Computational details

Molecular docking, one of the molecular modeling techniques, is widely exerted in drug design and discovery in structural molecular chemistry and biology. This technique helps to visualize the interaction between ligand and target, as well as to gain more insight information from experimental studies. Therefore, molecular docking simulation was utilized to describe the binding affinities and molecular interaction mechanisms of potential compounds (**2b, 2d, 2e, 3a, 3b, 3c** and **3e**) towards hCA I, hCA II, and α-Gly. Docking simulations were applied with AutoDock 4 [71] by selecting the first four structures with the highest efficiency among the results of biological activity analysis against the related targets. They were prepared by minimizing their energies at MOG [72] using PM6 parameters of SCIGRESS [73]. Then, crystal structures of available enzymes were downloaded from the protein database [74], the details of which are in our previous work [75], and prepared and minimized with CHARMm [76] force field by using DS 3.5 software [77]. The binding sites of the current target models were also edited and defined with the grid size of 80 × 80 × 80 Å via the same previous

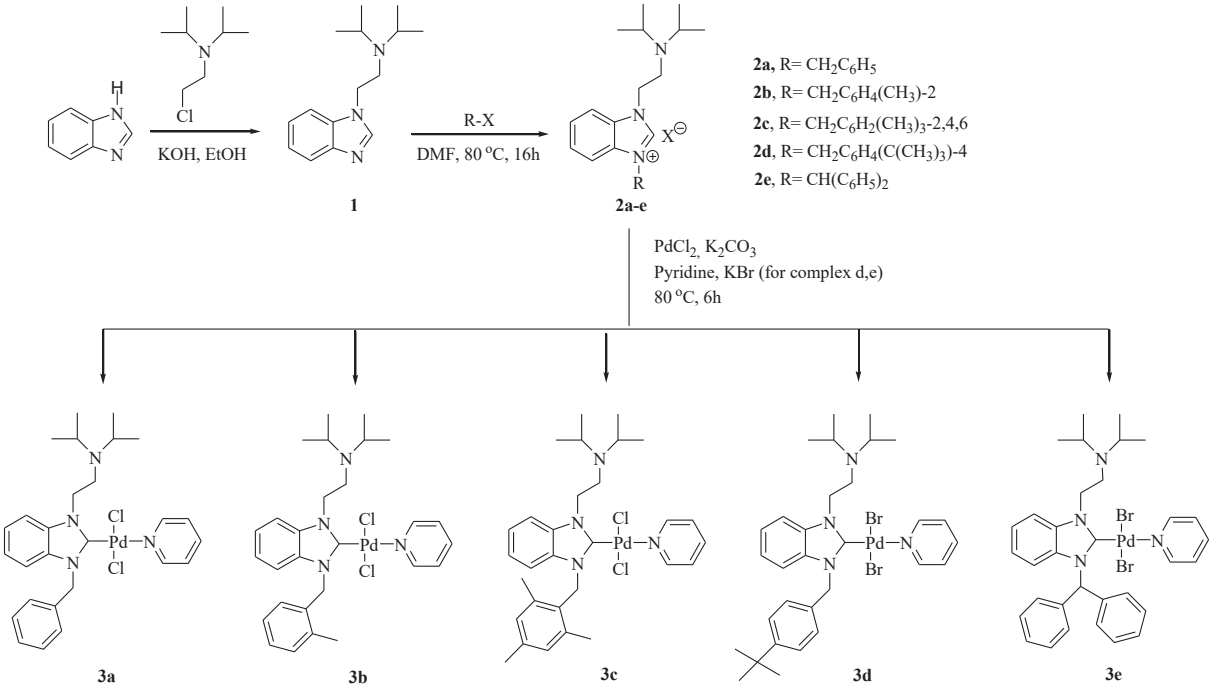

Scheme 1. The synthesis and structures of palladium complexes.

software. Finally, the prepared structures (the respective ligands) were docked with hCA I, hCA II, and α-Gly, and also analyzed for signifying the interaction feasibilities based on the enzyme inhibition results. The possible docking complexes were visualized and evaluated for detailed interactions via DS 3.5. Furthermore, acetazolamide (AZA) for hCA I and hCA II; and acarbose (ACR) for α-Gly were used as positive controls to validate the computational data occurring in this study by comparison with experimental data.

2.6. Bioactivity assays

These are the solutions used in the determination of ca enzyme esterase: Esterase activity buffer Tris-SO_4 (1 L, pH 7.4), 6.055 g (0.05 M) Tris–base is weighed and dissolved in a beaker with 950 mL of distilled water. Adjust pH 7.4 with 1 N H_2SO_4. Then, the solution is transferred to a 1 L balloon jug and the volume is made up to 1 L with distilled water. Also, p-nitrophenol acetate (PNA) substrate solution 50 mL: Weigh out 27.2 mg of ester and dissolve in 1 mL of DMSO [78]. Then, it is transferred to a 50 mL flask and the volume is made up to 50 mL with distilled water. The spectrophotometer was zeroed with Tris-SO_4 buffer solution. After the solution was prepared with 400 μL Tris-SO_4 buffer, 360 μL PNA substrate, 20 μL CA enzyme, necessary inhibitor and 220 μL distilled water, the absorbance amount was read each minute, and the absorbance amount was read at the end of 3 min (Total: 1000 μL). The absorbance difference was taken by reading the absorbance at 348 nm at 25 °C. The substrate (PNA) used in the experiments is prepared fresh daily. Activity measurements during kinetic studies were carried out with the esterase activity of the enzyme using Verport assay [79]. Additionally, *α*-glycosidase inhibitory effects of novel compunds **2a-e** and **3a-e** were determined according to the reported method by Tao *et al.* [80]. Moreover, the inhibitory effect of these novel complexes on the activity of the α-glycosidase enzyme was investigated utilizing the p-nitrophenyl-ᴅ-glycopyranoside substrate (p-NPG) as substrate. First, 200 μL of phosphate buffer was mixed with 40 μL of enzyme in phosphate buffer (0.15 U / mL, pH 4.7). Moreover, after preincubation, 50 μL of p-NPG was added to phosphate buffer (5 mM, pH 7.4) and incubated again at 30 °C. The absorbance was spectrophotometrically measured at 405 nm [81]**.** In the inhibitor study, activity measurements were made at different inhibitor concentrations. IC_{50} values were determined from the equation of the curve by plotting the activity (%) graphs of the inhibitors by the measured activity values. Lineweaver-Burk plots were drawn and K_i values were calculated from this chart [81].

3. Results and discussion

3.1. Synthesis of palladium(II)–NHC complexes

In this study, the benzimidazolium salts **2a-e** were synthesized by the two-step procedure previously described in literature as shown in Scheme 1. The reaction of benzimidazole with 2-diisopropylaminoethyl chloride at room temperature gave the 1-(2-diisopropylaminoethyl) benzimidazole, which on further alkylation with variety of alkyl halides in N,*N*-dimethylformamide at 80 °C afforded the benzimidazolium salts **2a-e**. Subsequent treatment of the benzimidazolium salts with $PdCl_2$ in the presence of K_2CO_3 as the base in pyridine at 80 °C afforded the (NHC)PdX_2(pyridine) complexes **3a-e.** After purification, palladium complexes were isolated as yellow solids in good yields of 68–84 %. A single crystal of **3b** for X-ray diffraction analysis was obtained from slow vapor diffusion of diethyl ether into a dichloromethane solution at room temperature. The prepared complexes are easily soluble in polar organic solvents such as dimethylsulfoxide, dichloromethane and chloroform, and insoluble in pentane, hexane, diethyl ether and toluene. These complexes are very stable both in solution and in solid states against air, light and moisture. The stability of the complexes was tested for 11 days by UV and ^{1}H NMR spectroscopy, and it was seen that (NHC) PdX_2(pyridine) complexes showed high stability without structural decomposition in the aqueous medium. The structure of palladium complexes was determined by elemental analysis, ^{1}H NMR, ^{13}C NMR, IR spectroscopy, mass spectrometry and the single crystal X-ray diffraction studies, which support the proposed structures. The palladium complexes exhibit characteristic υ(C═N) bands at 1411.7, 1404.9, 1403.3, 1409.1 and 1403.0 cm^{-1} respectively for **3a-e**. NMR analyses of complexes **3a-e** show that both the *N*-heterocyclic carbene and pyridine ligands have coordinated to palladium. The characteristic signals for the *C*2-proton of benzimidazolium salts were not observed in the ^{1}H NMR spectra of palladium complexes **3a-e**. Also, the characteristic *C*2-carbon

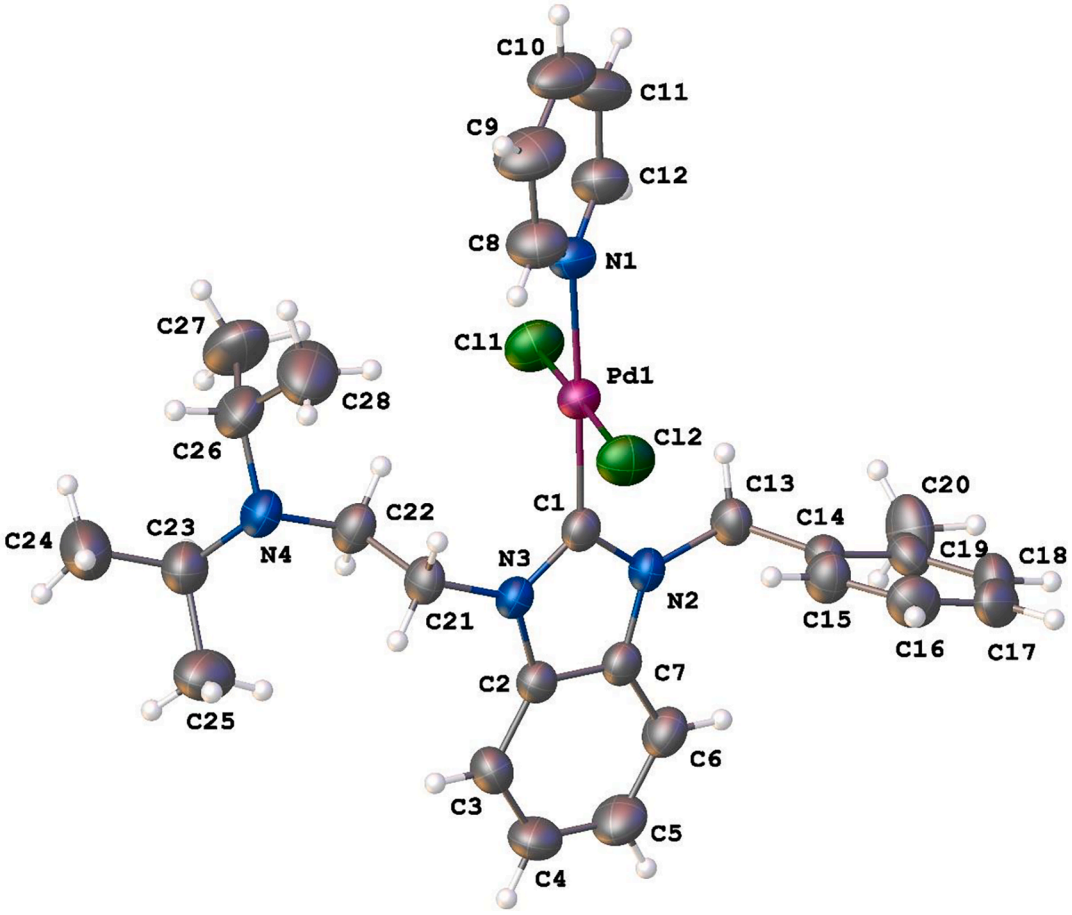

Fig. 1. Representation of the molecular structure of complex **3b** showing the non-H atom numbering scheme and drawn at the 50% probability level. Selected bond parameters (Å,°): Pd1–Cl1 2.2933(7), Pd1–Cl2 2.2932(7), Pd1–N1 2.117(2), Pd1–C1 1.953(3), C1–N2 1.348(3), C1–N3 1.348(3); Cl1–Pd1–Cl2 176.58(3), N1–Pd1–Cl1 91.81(7), N1–Pd1–Cl2 91.56(7), C1–Pd1–Cl1 88.71(7), C1–Pd1–Cl2 87.95(7), C1–Pd1–N1 177.88(10), N2–C1–N3 106.8(2).

signals of benzimidazolium salts were shifted to significantly lower field in the ^{13}C NMR spectra of palladium complexes **3a-e**. The ^{13}C NMR chemical shifts provide a useful diagnostic tool for this type of metal carbene complexes. The characteristic resonance of the carbene carbon was observed at 163.90, 164.14, 163.46, 163.40 and 167.70 ppm, respectively for **3a-e**, and these values agree with previously reported (NHC)PdX_2(pyridine) complexes [82]. Also, the elemental and mass analysis results of complexes **3a-e** are well-suited with the theoretical data.

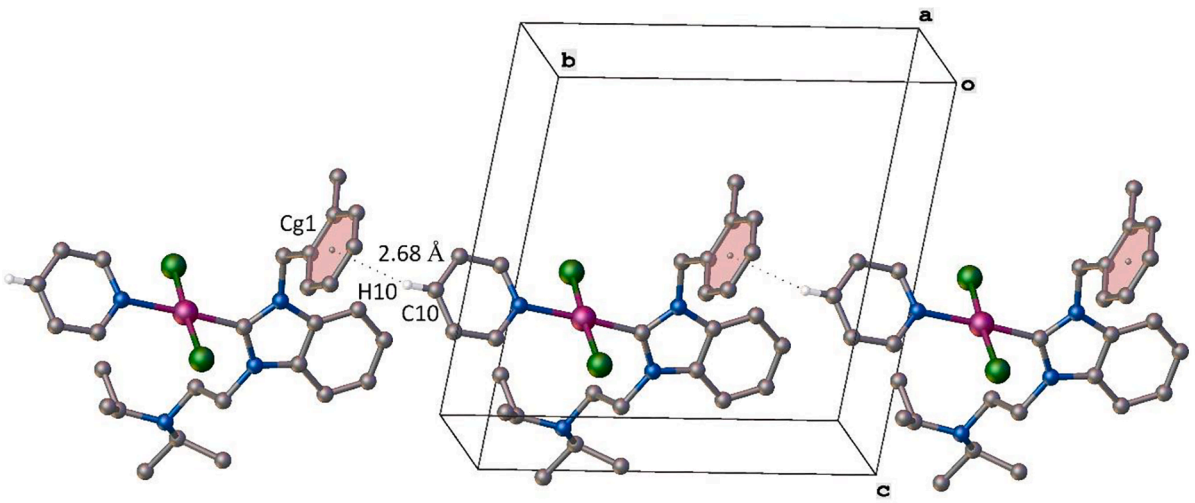

Fig. 2. Representation of a C—H···π stacking interactions along the *b* axis of complex **3b**. Cg1 represents the centroid of the C14–19 ring. Hydrogen atoms not involved in the interactions have been omitted for clarity.

Table 1
Inhibition results of benzimidazolium salts and palladium(II) complexes on some enzymes.

Compounds	IC_{50}						K_i		
	hCA I (μM)	r^2	hCA II (μM)	r^2	α-Gly (nM)	r^2	hCA I (μM)	hCA II (μM)	α-Gly (nM)
2a	67.81	0.9821	61.30	0.9832	346.54	0.9489	65.50 ± 8.20	57.60 ± 6.41	353.23 ± 29.24
2b	49.48	0.9441	46.85	0.9967	256.16	0.9519	46.56 ± 6.36	44.16 ± 5. 42	262.25 ± 15.64
2c	59.30	0.9838	57.63	0.9827	491.14	0.9666	57.92 ± 9. 53	54.22 ± 8.21	509.21 ± 26.61
2d	44.08	0.9184	38.83	0.9531	382.37	0.9506	41.62 ± 5.05	36.24 ± 3.58	391.65 ± 18.74
2e	48.15	0.9754	42.13	0.9818	238.90	0.9941	45.60 ± 4.24	40.88 ± 2.11	245.37 ± 12.91
3a	3.03	0.9942	2.70	0.9646	165.42	0.9936	2.75 ± 0.16	2.35 ± 0.20	171.60 ± 9.40
3b	1.95	0.9618	1.46	0.9380	192.51	0.9574	1.89 ± 0.15	1.30 ± 0.26	200.25 ± 10.21
3c	7.08	0.9613	6.48	0.9298	115.35	0.9991	7.02 ± 0.50	6.31 ± 0.16	118.86 ± 11.92
3d	7.32	0.9836	7.03	0.9732	206.48	0.9424	6.97 ± 1.04	6.87 ± 0.54	215.62 ± 22.74
3e	1.37	0.9839	1.14	0.9251	201.38	0.9854	1.17 ± 0.11	1.02 ± 0.08	273.43 ± 11.26
AZA[¥]	168.66	0.9875	191.28	0.9270	–	–	170.59 ± 49.17	203.31 ± 30.01	–
ACR[€]	–	–	–	–	375.38	–	–	–	436.41

[¥] [90].
[€] [100,101].

3.2. Structural description of complex 3b

The single-crystal X-ray structural studies reveal that the bimy–$PdCl_2$–py PEPPSI complex **3b** crystallizes in the triclinic space group $P\bar{1}$, and the component contains a Pd^{II} center, surrounded by a carbene carbon atom of the bimy type NHC ligand, a pyridine ligand, two chloride anions, forming a distorted four-coordinate *square planar* structure. The molecular structure of the complex is depicted in Fig. 1. Similar to Addison and Reedijk's five-coordination geometry index, Houser and co-workers developed geometry indexes τ_4 and $\tau_4^{'}$ to describe the geometries of four-coordinate complexes [83]. These structural indexes are;

$$\tau_4 = \frac{360^{\circ} - (\alpha + \beta)}{360^{\circ} - 2\theta}$$

$$\tau_{4'} = \frac{\beta - \alpha}{360^{\circ} - \theta} + \frac{180^{\circ} - \beta}{180^{\circ} - \theta}$$

where α and β ($\beta > \alpha$) are the two greatest valence angles and θ is the ideal tetrahedral angle (109.5°). For an ideal *square planar* geometry, the τ_4 and $\tau_{4'}$ values are 0, while for a perfect *tetrahedral* geometry they are 1. The four-coordinate geometry indexes τ_4 and $\tau_{4'}$ of the complex **3b** are calculated to be 0.039 and 0.035, respectively, verifying a slightly distorted *square planar* geometry. Around the metal center, the *N*-benzimidazole moiety has a strong twist that makes it almost perpendicular to the coordination plane with a dihedral angle of 74.31°. This situation is typical for NHC complexes to reduce steric congestion. The Pd–$C_{carbene}$ bond length [1.953(3) Å] is smaller than the sum of the individual covalent radii of the palladium and carbon atoms (2.12 Å) [84], but is similar to the related bimy–$PdCl_2$–py complexes [50,85,86]. The Pd–N_{py} bond length [2.117(2) Å] is further extended, which is attributed to the *trans* effect of NHC ligand [87]. The Pd–Cl bond distances are shorter than the sum of the individual covalent radii (2.41 Å), but compatible with the similar bimy–$PdCl_2$–py complexes in the literature [88,89]. In the crystal structure of the complex, molecules are held together by weak intramolecular C—H···Cl interactions, a C—H···π stacking interaction that is C10–*H*10···Cg1^{i} [*H*10···Cg1 = 2.68 Å, C10···Cg1 = 3.587(4), C10–*H*10···Cg1 = 166°, symmetry code (i) ×, 1 + y, z], and van der Waals forces. Fig. 2 illustrates the partial view of the crystal packing of the complex *via* the C—H···π stacking interactions.

3.3. Enzymes inhibition results

Among all tested compounds **2a-e** and **3a-e**, complex **3e** (hCA I, K_i = 1.17 ± 0.11 μM; IC_{50} = 1.37 μM with r^2: 0.9839) having benzhydryl group was recognized as the most potent inhibitor of hCA I isoform when compared with the standard acetazolamide (K_i = 170.59 ± 49.17 μM) [90]. However, **2a** containing benzyl group (hCA I, K_i = 65.50 ± 8.20 μM; IC_{50} = 67.81 μM with r^2: 0.9821) showed less inhibitory potential against the target as compared to other compounds. Comparing the inhibition abilities of complexes **3a** and **3b** (hCA I, K_i = 2.75 ± 0.16 μM; K_i = 1.89 ± 0.15 μM) reveals that inclusion of methyl group at 2-position of the phenyl ring increases the inhibitory potential against the hCA I isoform. Between benzimidazolium salts **2a-e**, salt **2d** (hCA I, K_i = 41.62 ± 5.05 μM; IC_{50} = 44.08 μM with r^2: 0.9184) having 4-tertbutylbenzyl group was the first potent analog of the **2a-e** series. Nonetheless, the presence of benzhydryl group in analog **3e** (hCA II, K_i = 1.02 ± 0.08 μM; IC_{50} = 1.14 μM with r^2: 0.9251) presented the best decrease in hCA II inhibitory potential (Table 1). Furthermore, most of compounds **2a-e** and **3a-e** showed good inhibitory potential against hCA II isoform. Two classes of CA inhibitors are studied; 1) Inorganic anions complexing with metals 2) Sulfonamides. The most potent organic inhibitors of the CA enzyme; are heteroaromatic sulfonamides and aromatics [91]. The chemical structure of sulfonamides is R-SO_2NH_2. where R is usually heteroaromatic or aromatic ring systems. The inhibition effect of sulfonamides on the CA enzyme is extremely important because sulfonamides can easily acquire ionic structure. In addition to this hydrophilic region, sulfonamides also have aromatic and heteroaromatic hydrophobic regions. The importance of CA inhibitors in the diagnosis and treatment of diseases has been revealed as a result of inhibition studies on the CA enzyme for the treatment of glaucoma [92]. In the aforementioned studies, besides elucidating the catalysis mechanisms of the CA enzyme, the distribution of this enzyme to the tissues and its vital functions in these tissues were understood, and as a result, the synthesis of the inhibitors and activities of the CA enzyme was accelerated. In these studies, a wide variety of CA enzyme inhibitors were synthesized, and these inhibitors are primarily drugs in the treatment of glaucoma, drugs in epilepsy, painkillers, antitumor and neurological disorders, diagnostic material in positron emission tomography and magnetic resonance determination, antiulcer and diuretic drugs. It is still used in clinics as a guide and antibiotic in its development. For this reason, knowing the inhibition mechanism of the CA enzyme and synthesizing new compounds have gained great importance [93,94]. Recently, many studies on CA inhibition of *N*-heterocyclic carbene complexes have been conducted by our group. In a study in this context, some novel morpholine liganded Pd-based NHC complexes inhibited cytosolic hCAs I and II isozymes with Ki values in the range of 10.77–45.86 and 25.42–57.82 μM, respectively [95]. Similarly, novel 2-aminopyridine liganded Pd(II) NHC complexes had inhibition effects on both CA isoforms with Ki values between 5.78 and 22.51 and 13.77–30.81 nM, respectively [51]. In a recent study, a novel Ag-NHC complex bearing the hydroxyethyl ligand demonstrated hCAs I and II isozyme inhibition effects with K_is of 1.14 0.26 μM against hCA I and 1.88 μM against hCA II [96]. In the same manner, some dative donor ligand NHC precursors and

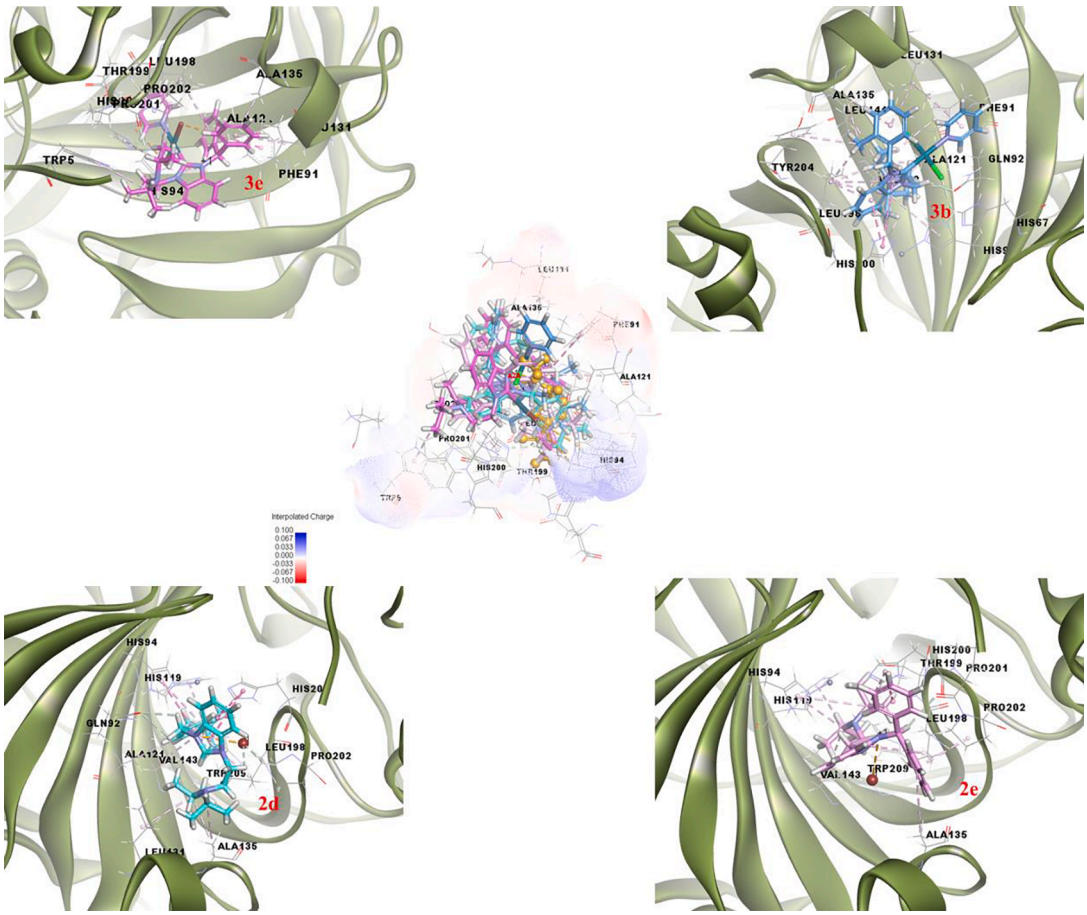

Fig. 3. Superimposed form of compounds **3e, 3b, 2d** and **2e** (pink, blue, cyan and light pink colour, stick form), **AZA** (orange, ball and stick form) as control compound with **hCA I**, respectively.

their Ag(I)NHC coordination compounds had K_is in the range of 1.00–2.31 μM for hCA I, 1.30–2.85 μM for hCA II isoenzyme [97]. Also, novel silver(I)NHC complexes bearing 2-(4-hydroxyphenyl)ethyl group demonstrated efficient CA I and II inhibition profile with Ki values ranging of 5.45–24.35 and 8.99–22.98 μM towards hCAs I and II isozymes [98]. In another influential study, silver NHC complexes bearing fluorinated benzyl group showed Ki values ranging of 66.01–135.23 and 62.53–136.97 μM towards both hCAs, respectively [99].

Newly synthesized complexes were also evaluated against α-glycosidase (Table 1). The obtained data demonstrated that some of the complexes with K_i values ranging from 118.86 ± 11.92 to 509.21 ± 26.61 nM exhibited inhibitory ability more than positive control acarbose with K_i value of 436.41 μM [100,101]. Among the synthesized compounds, the most potent compounds were **3c** with K_i values of 118.86 ± 11.92 nM between palladium(II) complexes **3a-e** and **2e** with K_i values of 245.37 ± 12.91 nM between benzimidazolium salts **2a-e**. The most of complexes were two folds more potent than positive control acarbose. The α-glycosidase enzyme is a carbohydrate digestive that is located in the small intestine, and catalyzes the cleavage of α-glucopyranoside bond in oligosaccharide molecules and disaccharide molecules, leading to increases in blood glucose concentration. Inhibitors of this enzyme, therefore, delay the digestion of carbohydrate molecules and their subsequent absorption [102]. Recently, diverse studies have been performed to investigate natural products such as α-glycosidase inhibitors with acarbose showing perfect potential and clinically used as a first-line drug for treating Type 2-diabetes (T2DM). Non-insulin-dependent T2DM takes up 90 % of total diabetes mellitus cases in the current world. Indeed, carbohydrate metabolic enzymes can hydrolyze oligosaccharides into glucose. By inhibiting the activities of these metabolic enzymes, the absorption of glucose in the intestine was slowed down, and the blood sugar level can be well managed. Two α-glycosidase inhibitors drugs, namely voglibose and acarbose have been extensively utilized in the control of postprandial hyperglycemia [103]. Recently, metal compounds have attracted important attention. Based on this background, an extensive diversity of metal-containing factors has been suggested demonstrating important anticancer and antimicrobial as well as anti-diabetic power. The encouraging α-glycosidase inhibitory studies of copper, palladium, and cobalt complexes stimulate further optimization of such scaffolds [104]. For example, metal complexes of 1-amidino-O-alkylureas have been recorded because of their raised biochemical activities. These complexes can chelate with diverse structural kinds and various metal ions. Different metal complexes of Zn(II), Ni(II), and Cu(II) have shown a considerable increase in hypoglycemic activity when compared to pure metformin drugs [105]. Lately, diverse metformin complexes of Fe(III), Mn(II), Ni(II), Cr(III), Zn (II), Cd(II), Mg(II), Cu(II), Ba(II), Sr(II), and Au(III) were designed and synthesized as an anti-diabetic drug model [106]. Additionally, α-glycosidase inhibitor compounds are used as anti-HIV, anti-cancer, and anti-hepatitis drugs. Also, complexes **3c** and **3a** showed good inhibitory potential with Ki values of 118.86 ± 11.92 nM and 171.60 ± 9.40 nM against α-glycosidase. Recent inhibition studies on α-glycosidase have shown that this enzyme is effectively inhibited by some novel morpholine liganded Pd-based *N*-heterocyclic carbene complexes with K_i values in the range of 12.26–50.36 mM [95]. In another study, novel 2-aminopyridine liganded Pd(II) *N*-heterocyclic carbene complexes had inhibition effects on α-glycosidase with K_is between 4.44 and 12.67 nM [51]. In our recent study, a novel Ag-*N*-heterocyclic carbene complex bearing the hydroxyethyl ligand exhibited α-glycosidase with a Ki value

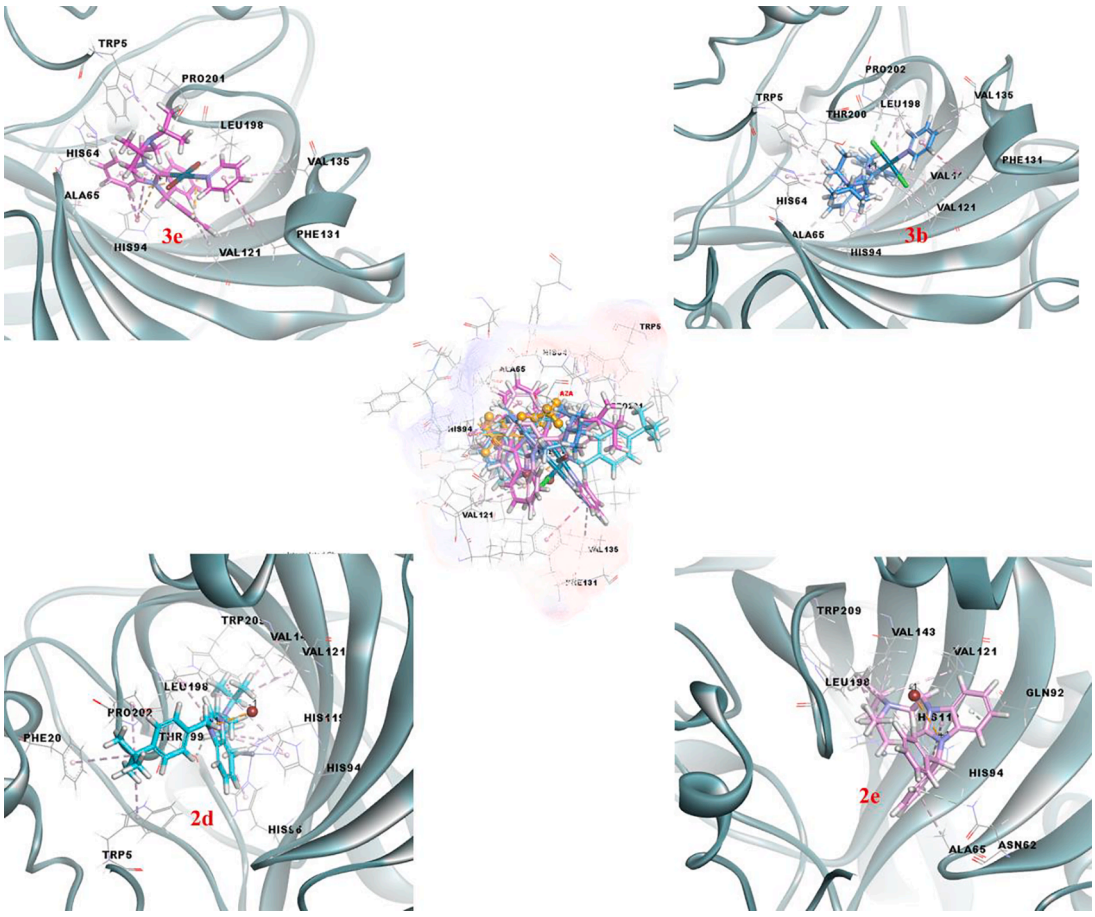

Fig. 4. Superimposed form of compounds **3e, 3b, 2d** and **2e** (pink, blue, cyan and light pink colour, stick form), **AZA** (orange, ball and stick form) as control compound with **hCA II**, respectively.

of 10.75 μM [96]. Also, novel silver(I)*N*-heterocyclic carbene complexes bearing 2-(4-hydroxyphenyl)ethyl group showed Ki values ranging of 3.09–13.86 μM towards α-glycosidase, which were found in the brush border of the small intestine that hydrolysis α(1 → 4) bonds [98]. In another study, silver NHC complexes bearing fluorinated benzyl group showed Ki values ranging of 17.83–211.54 μM on α-glycosidase [99].

3.4. Molecular docking

Based on the selected targets, the biochemical relationships of **2b, 2d, 2e, 3a, 3b, 3c** and **3e** compounds were calculated and evaluated with the aid of in silico molecular docking. As a result of the docking, the interaction mechanism for hCA I, hCA II, and α-Gly in the active region of the target proteins and which types of non-binding interactions take place are indicated in three dimensions. Docking conformations of the respective compounds and the controls against the respective targets are presented in Figs. 3-5. Details of potential complexes formed are listed in Table S2. The binding energy values of the respective compounds for target proteins are also given in Table 2.

As a result of the inhibition analysis performed against carbonic anhydrase I and II enzymes, the four compounds with the highest inhibition ability are compounds **3e, 3b, 2d** and **2e**, respectively. Molecular coupling studies of these compounds with both target enzymes show similar results, but the activities of the related compounds against the hCA II target are better against the hCA I isoenzyme. Compound **3e** (-7.81 kcal/mol; 1.88 μM), **3b** (-7.54 kcal/mol; 2.97 μM), **2d** (-6.84 kcal/mol; 9.70 μM) and **2e** (-6.56 kcal/mol; 15.56 μM), respectively In Table 2, they show the best binding affinity and inhibitor constant values with the target enzyme hCA I. In addition, Fig. 3 shows that for the present targets, the four active molecules of interest bind and interact better with hCA I than with the control compound Acetazolamide (AZA, Figure S18).

The same compounds (**3e, 3b, 2d** and **2e**) show similar results towards the second target enzyme, hCA II, but show stronger interactions and a resulting better binding affinity, summarized in Table 2. The compound **3e** forms one H-bonds with Pro20; four electrostatic interactions with Zn metal, His94, and Br^- ion, and also eleven hydrophobic interactions with His94, Phe131, Trp5, His64, Ala65, Val121, Leu198 and Val135 residues of hCA II. Next second compound, **3b** generates two hydrogen bonds (Pro202 and Thr200), one electrostatic interaction (Zn metal) and fourteen hydrophobic interactions (His94, Phe131, Val121, Leu198, Trp5, His64, Ala65, Val135, Pro202, Val121 and Val143). Another one, compound **2d** makes a hydrogen bond with Br^- ion and Thr199, one electrostatic (Br- ion), and hydrophobic interactions with Pro202, Val121, Val143, Leu198, Trp5, Phe20, His94, His96, His119, Trp209 and Leu198 residues, as given in Fig. 4. The last compound, **2e** forms three hydrogen bonds with Br- ion, Asn62 and Gln92; one electrostatic interaction with Br- ion and ten hydrophobic interactions with His94, Val121, Val143, Leu198, His94, His119, Trp209 and Ala65 residues of the active site in hCA II. The above findings show that the apolar region interaction is more favored in the active region of both targets than in the polar region. Electrostatic interactions with Zn seem to have a dominant effect on the inhibition ability order of the related compounds compared to hydrogen bonding and hydrophobic interactions with target structures. In addition, we should not ignore the importance of the binding orientations of the compounds in the active site in their activity.

Besides these, acarbose as a positive control was docked with α-Gly.

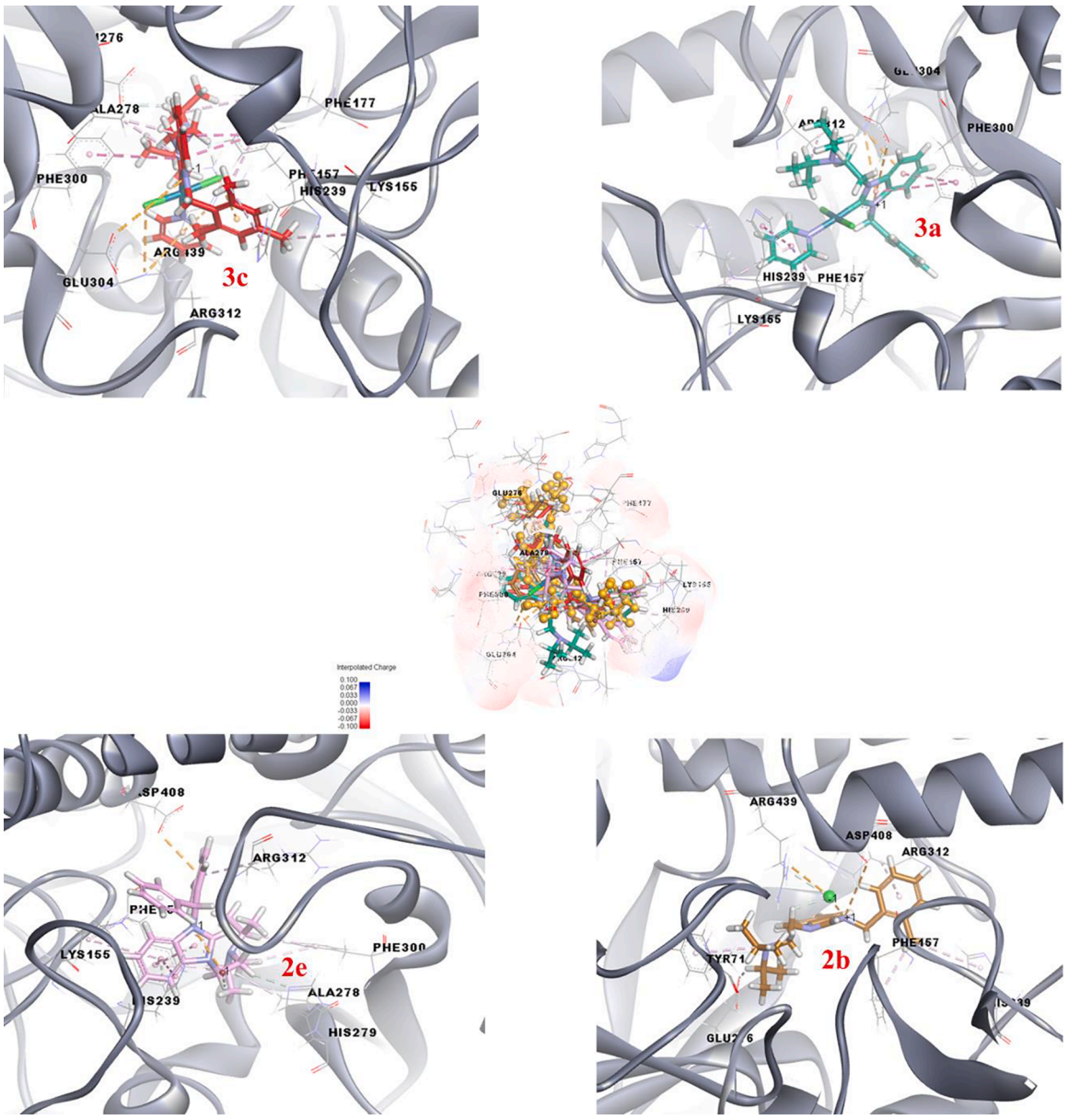

Fig. 5. Superimposed form of compounds **3c, 3a, 2e** and **2b** (red, green, light pink and brown colour, stick form), and **ACR** (orange, ball and stick form) as control compound with **α-Gly**, respectively.

The results present the interaction mechanism and which type of non-bonding interactions involved in the binding site of α-glycosidase. In docking studies, the potential compounds **3c, 3a, 2e** and **2b** were applied to the same process based on the current control. Their binding affinity was likewise calculated and matched with acarbose as α-glycosidase inhibitor in Table 2**.**

Residues of the target structure Arg212, Asn241, Ser156, Glu304, Glu276, Asp68, His348, Asp349 and Asp214 and the control compound acarbose form nineteen hydrogen bonds. The three-dimensional (3D) orientation and details of acarbose are indicated in Figure S20 and Table S2 in the supplementary information section of the study.

The current compounds **3c, 3a, 2e** and **2b** were docked with α-glycosidase. These compounds have better affinity than the control compound, acarbose (-7.53 kcal /mol). The compound **3c** which is the best one (BE: −9.87 kcal/mol), has four electrostatic (Arg312, Glu304, and Arg439), one hydrogen bond with Glu276 and ten hydrophobic interactions with Phe157, Phe300, Lys155, Phe177, His239, Ala278 and Arg439 residues of α-glycosidase, (Fig. 5). The second compound, **3a** forms two hydrogen bonds with Glu304; three electrostatic interactions with Glu304, and Arg312. Further, Phe157, Phe300, His239, Arg312 and Lys155 residues in the active site of α-glycosidase have six hydrophobic interactions with the respective compound. Next compound, **2e** has third better affinity against the α-glycosidase target (-9.04 kcal/mol). It has three hydrogen bonds, two electrostatic, and ten hydrophobic interactions with Br^- ion, His279, Asp408, His239, Phe157, Ala278, Phe300, Lys155 and Arg312 residues in the binding site of the target model. The last compound **2b** makes three electrostatic, three hydrogen bonds and four hydrophobic interactions with Arg439, Asp408, Cl^- ion, Glu276, Tyr71, Phe157, His239 and Arg312 amino acids of the α-glycosidase. Meanwhile, Fig. 5 shows that not only hydrogen bonds but also electrostatic and hydrophobic interactions of related compounds in α-glycosidase have a major contribution when compared with the control compound. Thus, the obtained data in the molecular docking processes also seem to support the eliciting and visualization of the findings of the inhibition assay.

In general, palladium complexes (**3a, 3b, 3c** and **3e**) against hCA I,

Table 2
The binding energy and inhibition constant values of the compounds (**2b, 2d, 2e, 3a, 3b, 3c** and **3e**), acetazolamide (AZA) for hCA I, and hCA II; and acarbose (ACR) for α-Gly as controls.

hCA I	Free binding energy (kcal/mol)	Ki (μM)
2d	−6.84	9.70
2e	−6.56	15.56
3b	−7.54	2.97
3e	−7.81	1.88
AZA	*−6.14*	*31.64*
hCA II	**Free binding energy (kcal/mol)**	**Ki (μM)**
2d	−8.39	0.70
2e	−7.57	2.82
3b	−8.74	0.39
3e	−8.80	0.35
AZA	*−6.56*	*15.59*
α-Gly	**Free binding energy (kcal/mol)**	**Ki (μM)**
2b	−8.63	0.47
2e	−9.04	0.24
3a	−9.77	0.07
3c	−9.87	0.06
ACR	*−7.53*	*3.02*

hCA II and α-glycosidase produce better binding affinity and interaction than benzimidazolium salts (**2b, 2d** and **2e**). In particular, the palladium complexes showing the best binding affinity towards the hCA I and hCA II target are compounds **3e** and **3b**, respectively. In contrast, the palladium complexes that bind best to α-glycosidase are compounds **3c** and **3a**. Even from the two aforementioned previous targets, the current complex structures indicated show a high binding affinity for α-glycosidase.

4. Conclusion

In summary, five novel (NHC)PdX_2(pyridine) complexes were readily prepared in good yields by the reaction of benzimidazolium salts with $PdCl_2$ in the presence of K_2CO_3 as base in pyridine. These complexes were characterized by spectroscopic methods. Also, the molecular and crystal structure of **3b** was determined by the single-crystal X-ray diffraction technique revealing that the metal environment of the complex has a slightly distorted square planar geometry. The crystal packing of the complex exhibits weak intermolecular C—H···Cl interactions and C—H···π stacking interactions. The benzimidazolium salts **2a-e** and their palladium(II) complexes **3a-e** were tested against hCA I, hCA II, and *α*-glycosidase enzymes. All compounds showed good inhibition effect against these enzymes. However, The palladium(II) complexes **3a-e** showed high inhibition effect against hCA I, hCA II, and *α*-glycosidase than those of *N*-heterocyclic carbene precursors **2a-e**. In addition, as a result of the investigation in molecular docking studies of the compounds showing potent inhibition ability based on in vitro analysis, it was observed that palladium complexes showed better inhibition ability for all three target structures against their precursors.

Declaration of Competing Interest

The authors declare that they have no known competing financial interests or personal relationships that could have appeared to influence the work reported in this paper.

Data availability

The authors do not have permission to share data.

Acknowledgement

We thank the Adiyaman University Research Fund (FEFMAP/2021-0001) for financial support of this work and Dokuz Eylül University for the use of the Oxford Rigaku Xcalibur Eos Diffractometer (purchased under University Research Grant No: 2010.KB.FEN.13). The authors thank Esin Akı Yalcin and the research group for technical assistance.

Appendix A. Supplementary data

Supplementary data to this article can be found online at https://doi.org/10.1016/j.ica.2022.121239.

References

[1] D. Jansenn-Müller, F. Glorius, Chem. Soc. Rev. 46 (2017) 4845–4854.
[2] K. Öfele, J. Organomet. Chem. 12 (1968) 42–43.
[3] H.W. Wanzlick, H.J. Schönherr, Angew. Chem., Int. Ed. Engl. 7 (1968) 141–142.
[4] D.J. Cardin, B. Çetinkaya, M.F. Lappert, L. Manojlovic-Muir, K.W. Muir, J. Chem. Soc., Chem. Commun. (1971) 400–401.
[5] A.J. Arduengo III, R.L. Harlow, M. Kline, J. Am. Chem. Soc. 113 (1991) 361–363.
[6] W.A. Herrmann, M. Elison, J. Fischer, C. Kocher, G.R.J. Artus, Angew. Chem. Int. Ed. 34 (1995) 2371–2374.
[7] B. Çetinkaya, E. Çetinkaya, H. Küçükbay, R. Durmaz, Arzneim. Forsch. Drug Res. 46 (1996) 821–823.
[8] A.D. Tanase, G.D. Frey, E. Herdtweck, S.D. Hoffmann, W.A. Herrmann, J. Organomet. Chem. 692 (2007) 3316–3327.
[9] S. Demir, M. Yiğit, İ. Özdemir, J. Organomet. Chem. 732 (2013) 21–26.
[10] B. Yiğit, M. Yiğit, İ. Özdemir, E. Çetinkaya, Heterocycles 81 (2010) 943–953.
[11] R. Kılınçarslan, M. Yiğit, İ. Özdemir, E. Çetinkaya, B. Çetinkaya, J. Heterocycl. Chem. 44 (2007) 69–73.
[12] D. Enders, K. Breuer, G. Raabe, J. Runsink, J.H. Teles, J.-P. Melder, K. Ebel, S. Brode, Angew. Chem. Int. Ed. Engl. 34 (1995) 1021.
[13] T. Sato, D. Yoshioka, Y. Hirose, S. Oi, J. Organomet. Chem. 753 (2014) 20.
[14] H. Valdes, D. Canseco-Gonzalez, J.M. German-Acacio, D. Morales-Morales, J. Organomet. Chem. 867 (2018) 51–54.
[15] E. Rufino-Felipe, H. Valdes, J.M. German-Acacio, V. Reyes-Marquez, D. Morales-Morales, J. Organomet. Chem. 921 (2020), 121364.
[16] E. Rufino-Felipe, R.N. Osorio-Yanez, M. Vera, H. Valdes, L. Gonzalez-Sebastian, A. Reyes-Sanchez, D. Morales-Morales, Polyhedron 204 (2021), 115220.
[17] L.A. Turcio-Garcia, H. Valdes, S. Hernandez-Ortega, D. Canseco-Gonzalez, D. Morales-Morales, New J. Chem. (2022), https://doi.org/10.1039/D2NJ02949A.
[18] P.N. Muskawar, S.S. Kumar, P.R. Bhagat, J. Mol. Catal. A: Chem. 380 (2013) 112–117.
[19] A.K. Lal, M.D. Milton, Sens. Actuators B 202 (2014) 257–262.
[20] R. Dang, Y. Wang, J. Zeng, Z. Huang, Z. Fei, P.J. Dyson, J. Mater. Chem. A 5 (2017) 13526–13534.
[21] D. Hernandez-Romero, S. Rosete-Luna, A. Lopez-Monteon, A. Chavez-Pina, N. Perez-Hernandez, J. Marroquin-Flores, A. Cruz-Navarro, G. Pesado-Gomez, D. Morales-Morales, R. Colorado-Peralta, Coord. Chem. Rev. 439 (2021), 213930.
[22] J.C. Paez-Franco M.R. Zermeno-Ortega C. M. de la O-Contreras, D. Canseco-Gonzalez, J. R. Parra-Unda, A. Avila-Sorrosa, R. G. Enriquez, J. M. German-Acacio, D. Morales-Morales, Pharmaceutics 14 2022 402.
[23] E. Rufino-Felipe, R. Colorado-Peralta, V. Reyes-Marquez, H. Valdes, D. Morales-Morales, Anti-Cancer Agents Med. Chem. 21 (2021) 938–948.
[24] A. Sanchez-Mora, H. Valdes, M.T. Ramirez-Apan, A. Nieto-Camacho, S. Hernandez-Ortega, D. Canseco-Gonzalez, D. Morales-Morales, Inorg. Chim. Acta 496 (2019), 119061.
[25] A.C. Hillier, G.A. Grasa, M.S. Viciu, H.M. Lee, C. Yang, S.P. Nolan, J. Organomet. Chem. 653 (2002) 69.
[26] F. Li, J.J. Hu, L.L. Koh, T.S.A. Hor, Dalton Trans. 39 (2010) 5231.
[27] F.E. Hahn, M.C. Jahnke, V. Gomez-Benitez, D. Morales-Morales, T. Pape, Organometallics 24 (2005) 6458.
[28] J.F. Hartwig, M. Kawatsura, S.I. Hauck, K.H. Shaughnessy, L.M. Alcazar-Roman, J. Org. Chem. 64 (1999) 5575.
[29] C.J. O'Brien, E.B. Kantchev, C. Valente, N. Hadei, G.A. Chass, A. Lough, A. C. Hopkinson, M.G. Organ, Chem. Eur. J. 12 (2006) 4743.
[30] C. Valente, S. Çalimsiz, K.H. Hoi, D. Mallik, M. Sayah, M.G. Organ, Angew. Chem. Int. Ed. 51 (2012) 3314.
[31] F. Martinez-Olid, R. Andres, J.C. Flores, P. Gomez-Sal, Eur. J. Inorg. Chem. (2015) 4076.
[32] Y. Zhang, V. Cesar, G. Lavigne, Eur. J. Org. Chem. (2015) 2042.
[33] F. Wang, L. Zhu, Y. Zhou, X. Bao, H.F. Schaefer III, Chem. Eur. J. 21 (2015) 4153.
[34] K.M. Hindi, M.J. Panzner, C.A. Tessier, C.L. Cannon, W.J. Youngs, Chem. Rev. 109 (2009) 3859–3884.
[35] M. Tacke, J. Organomet. Chem. 782 (2015) 17–21.
[36] M.L. Teyssot, A.S. Jarrousse, M. Manin, A. Chevry, S. Roche, F. Norre, C. Beaudoin, L. Morel, D. Boyer, R. Mahiou, A. Gautier, Dalton Trans. (2009) 6894–6902.
[37] W. Liu, R. Gust, Chem. Soc. Rev. 42 (2013) 755–773.

[38] I. Ott, Chapter Four-Metal N-heterocyclic carbene complexes in medicinal chemistry, Advances in Inorganic Chemistry, Vol. 75, pp. 121-148, Eds: P. J. Sadler, R. Van Eldik, Academic Press, Elsevier, 2020.
[39] S. Nayak, S.L. Gaonkar, ChemMedChem 16 (2021) 1360–1390.
[40] S.Y. Hussaini, R.A. Haque, M.R. Razali, J. Organomet. Chem. 882 (2019) 96–111.
[41] A. Gautier, F. Cisnetti, Metallomics 4 (2012) 23–32.
[42] H. Burmeister, P. Dietze, L. Preu, J.E. Bandow, I. Ott, Molecules 26 (2021) 4282.
[43] B. Çetinkaya, İ. Özdemir, B. Binbaşıoğlu, R. Durmaz, S. Günal, Arzneim. Forsch Drug Res. 49 (1999) 538–540.
[44] G. Dahm, C. Bailly, L. Karmazin, S. Bellemin-Laponnaz, J. Organomet. Chem. 794 (2015) 115–124.
[45] M. Mora, C. Gimeno, R. Visbal, Chem. Soc. Rev. 48 (2019) 447–462.
[46] G.A. Fernandez, M.S.V. Gurovic, N.L. Olivera, A.B. Chopa, G.F. Silbestri, J. Inorg. Biochem. 135 (2014) 54–57.
[47] X. Liang, S. Luan, Z. Yin, M. He, C. He, L. Yin, Y. Zou, Z. Yuan, L. Li, X. Song, C. Lv, W. Zang, Eur. J. Med. Chem. 157 (2018) 62–80.
[48] W. Zheng, Q. Zheng, C. Chen, H. Wang, Appl. Organomet. Chem. (2021) e6544.
[49] M. Kaloğlu, N. Kaloğlu, S. Günal, İ. Özdemir, J. Coord. Chem. 74 (2021) 3031–3047.
[50] S. Ray, R. Mohan, J.K. Singh, M.K. Samantaray, M.M. Shaikh, D. Panda, P. Ghosh, J. Am. Chem. Soc. 129 (2007) 15042–15053.
[51] F. Erdemir, D. Barut Celepci, A. Aktaş, Y. Gök, R. Kaya, P. Taslimi, Y. Demir, İ. Gülçin, Bioorg. Chem. 91 (2019), 103134.
[52] S. Bal, Ö. Demirci, B. Şen, P. Taslimi, A. Aktaş, Y. Gök, M. Aygün, İ. Gülçin, Polyhedron 198 (2021), 115060.
[53] S. Daşgın, Y. Gök, D. Barut Celepci, P. Taslimi, M. İzmirli, A. Aktaş, İ. Gülçin, J. Mol. Struct. 1228 (2021), 129442.
[54] Ç. Bayrak, P. Taslimi, İ. Gülçin, A. Menzek, Bioorg. Chem. 72 (2017) 359–366.
[55] A. Biçer, P. Taslimi, G. Yakalı, İ. Gülcin, M.S. Gültekin, G.T. Cin, Bioorg. Chem. 82 (2019) 393–404.
[56] Ç. Bayrak, P. Taslimi, H.S. Kahraman, İ. Gülçin, A. Menzek, Bioorg. Chem. 85 (2019) 128–139.
[57] K. Küçükoğlu, H.İ. Gül, P. Taslimi, İ. Gülçin, C.T. Supuran, Bioorg. Chem. 86 (2019) 316–321.
[58] F. Turkan, A. Çetin, P. Taslimi, M. Karaman, İ. Gülçin, Bioorg. Chem. 86 (2019) 420–427.
[59] M. Boztas, P. Taslimi, M.A. Yavari, İ. Gülçin, E. Sahin, A. Menzek, Bioorg. Chem. 89 (2019), 103017.
[60] D. Kısa, N. Korkmaz, P. Taslimi, B. Tuzun, Ş. Tekin, A. Karadag, F. Şen, Bioorg. Chem. 101 (2020), 104066.
[61] H. Genc Bilgicli, D. Ergon, P. Taslimi, B. Tüzün, İ. Akyazı Kuru, M. Zengin, İ. Gülçin, Bioorg. Chem. 101 (2020), 103969.
[62] P. Taslimi, K. Turhan, F. Türkan, H.S. Karaman, Z. Turgut, İ. Gulcin, Bioorg. Chem. 97 (2020), 103647.
[63] M. Yiğit, B. Yiğit, P. Taslimi, İ. Özdemir, M. Karaman, İ. Gülçin, J. Mol. Struct. 1207 (2020), 127802.
[64] Ü. Kızrak, O. Çiftçi, İ. Özdemir, N. Gürbüz, S. Demir Düşünceli, M. Kaloğlu, L. Mansour, F. Zaghrouba, N. Hamdi, İ. Özdemir, J. Organomet. Chem. 882 (2019) 26–32.
[65] D. Barut Celepci, B. Yiğit, M. Yiğit, İ. Özdemir, M. Aygün, J. Mol. Struct. 1239 (2021), 130460.
[66] CrysAlisPro Software, Version 1.171.41.93a, Rigaku Corporation, Oxford, UK. 2020.
[67] R.C. Clark, J.S. Reid, Acta Crystallogr. 51 (1995) 887–897.
[68] G.M. Sheldrick, Acta Crystallog. Sect. A 71 (2015) 3–8.
[69] A.L. Spek, Platon Acta. Cryst. A 46 (1990) 34.
[70] O.V. Dolomanov, L.J. Bourhis, R.J. Gildea, J.A.K. Howard, H. Puschmann, J. Appl. Cryst. 42 (2009) 339–341.
[71] G.M. Morris, R. Huey, W. Lindstrom, M.F. Sanner, R.K. Belew, D.S. Goodsell, J. Comput Chem. 30 (2009) 2785–2791.
[72] MO-G Version 1.2A, Fujitsu Limited, Tokyo, Japan, 2013.
[73] N. Marchand, P. Lienard, H. Siehl, H. Izato, Fujitsu Scientific & Technical Journal 50 (2014) 46–51.
[74] Y. Rose, J.M. Duarte, R. Lowe, J. Segura, C. Bi, C. Bhikadiya, L. Chen, A.S. Rose, S. Bittrich, S.K. Burley, J.D. Westbrook, J. Mol. Biol. 433 (2021), 166704.
[75] M.A. Ansari, S.M. Saad, K.M. Khan, U. Salar, P. Taslimi, T. Taskın-Tok, F. Saleem, S. Jahangir, Arch. Pharm. 355 (2022) 2100376.
[76] B.R. Brooks, R.E. Bruccoleri, B.D. Olafson, D.J. States, S. Swaminathan, M. Karplus, J. Comp. Chem. 4 (1983) 187–217.
[77] Accelrys Software Inc. Discovery Studio Modeling Environment, Release 3.5 Accelrys Software Inc, San Diego, 2013.
[78] İ. Gulçin, B. Trofimov, R. Kaya, P. Taslimi, L. Sobenina, E. Schmidt, O. Petrova, S. Malysheva, N. Gusarova, V. Farzaliyev, A. Sujayev, S. Alwasel, C.T. Supuran, Bioorg. Chem. 103 (2020), 104171.
[79] J.A. Verpoorte, S. Mehta, J.T. Edsall, J. Biol. Chem. 242 (1967) 4221–4229.
[80] Y. Tao, Y. Zhang, Y. Cheng, Y. Wang, Biomed. Chromatogr. 27 (2013) 148–155.
[81] A. Sujayev, P. Taslimi, E. Garibov, M. Karaman, M.M. Zangenehde, Bioorg. Chem. 104 (2020), 104216.
[82] H. Karabıyık, B. Yiğit, M. Yiğit, İ. Özdemir, H. Karabıyık, Acta Cryst. C 75 (2019) 1–10.
[83] L. Yang, D.R. Powell, R.P. Houser, Dalton Trans. (2007) 955–964.
[84] B. Cordero, V. Gomez, A.E. Platero-Prats, M. Reves, J. Echeverria, E. Cremades, F. Barragan, S. Alvarez, Dalton Trans. (2008) 2832–2838.
[85] N. Özdemir, N. Touj, S. Yaşar, N. Hamdi, İ. Özdemir, Mol. Cryst. Liq. Cryst. 714 (2021) 26–36.
[86] Z. Nawaz, N. Gürbüz, M.N. Zafar, M.N. Tahir, M. Ashfaq, H. Karci, I. Özdemir, Polyhedron 208 (2021), 115412.
[87] V. Dragutan, I. Dragutan, Platinum Metals Rev. 49 (2005) 183–188.
[88] N. Özdemir, M. Kaloğlu, N. Kaloğlu, N. Gürbüz, İ. Özdemir, Inorg. Nano-Met. Chem. 52 (2022) 493.
[89] I. Kılıç Cıkla N. Şahin N. Özdemir N. Gürbüz İ. Özdemir Russ. J. Phys. Chem. A 95 2021 84 92.
[90] O. Çakmak, S. Ökten, D. Alımlı, C.C. Ersanlı, P. Taslimi, Ü.A. Koçyiğit, J. Mol. Struct. 1220 (2020), 128666.
[91] S. Bal, R. Kaya, Y. Gök, P. Taslimi, A. Aktaş, M. Karaman, İ. Gülçin, Bioorg. Chem. 94 (2020), 103468.
[92] H.U. Çelebioglu, Y. Erden, F. Hamurcu, P. Taslimi, O.Ş. Şentürk, Ü. Özdemir Özmen, B. Tüzün, İ. Gülçin, J. Biomol. Struct. Dyn. 39 (2021) 5539–5550.
[93] P. Taslimi, C. Çağlayan, F. Farzaliyev, O. Nabiyev, A. Sujayev, F. Türkan, R. Kaya, İ. Gülçin, J. Biochem. Mol. Toxicol. 32 (2018) e22042.
[94] C. Yamali, H.İ. Gül, A. Ece, P. Taslimi, İ. Gülçin, Chem. Biol. Drug Des. 91 (2018) 854–866.
[95] A. Aktaş, D. Barut Celepci, R. Kaya, P. Taslimi, Y. Gök, M. Aygün, İ. Gülçin, Polyhedron 159 (2019) 345–354.
[96] A. Aktas, D. Barut Celepci, Y. Gök, P. Taslimi, H. Akıncıoğlu, İ. Gülçin, Crystals 10 (2020) 171.
[97] A. Kazancı, Y. Gök, R. Kaya, A. Aktaş, P. Taslimi, İ. Gülçin, Polyhedron 193 (2021), 114866.
[98] A. Behçet, A. Aktaş, Y. Gök, R. Kaya, P. Taslimi, İ. Gülçin, J. Heterocycl. Chem. 58 (2021) 603–611.
[99] S. Bal, Ö. Demirci, B. Şen, T. Taşkın Tok, P. Taslimi, A. Aktaş, Y. Gök, M. Aygün, İ. Gülçin, Appl. Organomet. Chem. 35 (2021) e6312.
[100] Q.N. Tariq, S. Malik, M.M. Naseer, S.U. Khan, A. Ashraf, M. Ashraf, M. Rafiq, K. Mahmood, M.N. Tahir, S. Shafiq, Bioorg. Chem. 84 (2019) 372–383.
[101] V.G. Klochkov, E.N. Bezsonova, M. Dubar, D.D. Melekhina, V.V. Temnov, E. V. Zaryanova, N.A. Lozinskaya, D.A. Babkov, A.A. Spasov, Bioorg. Med. Chem. Lett. 55 (2022), 128449.
[102] S. Rajendrachari, P. Taslimi, A.C. Karaoglanli, O. Uzun, E. Alp, G.K. Jayaprakash, Arab. J. Chem. 14 (2021), 103180.
[103] M. Sertçelik, F.E. Öztürkkan Özbek, P. Taslimi, H. Necefoglu, T. Hökelek, Appl. Organomet. Chem. 35 (2021) e6182.
[104] S.N. Kertmen, I. Gonul, M. Kose, J. Mol. Struct. 1152 (2018) 29–36.
[105] A.M.A. Adam, T. Sharshar, M.A. Mohamed, O.B. Ibrahim, M.S. Refat, Spectrochim. Acta A Mol. Biomol. Spectrosc. 149 (2015) 323–332.
[106] B. Krishan, S.A. Iqbal, J. Chem. (2014).